

<https://helda.helsinki.fi>

---

## Experimental observation of two-photon photoelectric effect from silver aerosol nanoparticles

Sipilä, M.

2007

---

Sipilä , M , Lushnikov , A A , Khriachtchev , L , Kulmala , M , Tervahattu , H & Räsänen , M  
2007 , ' Experimental observation of two-photon photoelectric effect from silver aerosol  
nanoparticles ' , New Journal of Physics , vol. 9 , pp. 368-375 . <https://doi.org/10.1088/1367-2630/9/10/368>

---

<http://hdl.handle.net/10138/166266>

<https://doi.org/10.1088/1367-2630/9/10/368>

---

cc\_by

publishedVersion

---

*Downloaded from Helda, University of Helsinki institutional repository.*

*This is an electronic reprint of the original article.*

*This reprint may differ from the original in pagination and typographic detail.*

*Please cite the original version.*

## Experimental observation of two-photon photoelectric effect from silver aerosol nanoparticles

This content has been downloaded from IOPscience. Please scroll down to see the full text.

2007 New J. Phys. 9 368

(<http://iopscience.iop.org/1367-2630/9/10/368>)

View [the table of contents for this issue](#), or go to the [journal homepage](#) for more

### Download details:

IP Address: 128.214.163.21

This content was downloaded on 29/08/2016 at 12:25

Please note that [terms and conditions apply](#).

You may also be interested in:

[Nanoscopic Electrofocusing for Bio-Nanoelectronic Devices: Experimental methods and results for the nanoscopic lens](#)

S Lakshmanan and M R Hamblin

[Single metal nanoparticles](#)

P Zijlstra and M Orrit

[Nonlinear optical response of germanium nanoparticles](#)

Manoj Kumar, A K Shukla, H S Mavi et al.

[A radial differential mobility analyzer for the size-classification of gas-phase synthesized nanoparticles at low pressures](#)

K K Nanda and F E Kruis

[Spatial and size-resolved electrostatic-directed deposition of nanoparticles on a field-generating substrate: theoretical and experimental analysis](#)

D-H Tsai, T Hawa, H-C Kan et al.

[Ultrabright and efficient single-photon generation based on nitrogen-vacancy centres in nanodiamonds on a solid immersion lens](#)

Tim Schröder, Friedemann Gädeke, Moritz Julian Banholzer et al.

## Experimental observation of two-photon photoelectric effect from silver aerosol nanoparticles

M Sipilä<sup>1</sup>, A A Lushnikov<sup>1</sup>, L Khriachtchev<sup>2</sup>, M Kulmala<sup>1</sup>,  
H Tervahattu<sup>3</sup> and M Räsänen<sup>2</sup>

<sup>1</sup> Department of Physical Sciences, University of Helsinki, PO Box 64,  
FIN-00014, Helsinki, Finland

<sup>2</sup> Laboratory of Physical Chemistry, University of Helsinki, PO Box 55,  
FIN-00014, Helsinki, Finland

<sup>3</sup> Department of Biological and Environmental Sciences, University of Helsinki,  
PO Box 27, FIN-00014 Helsinki, Finland

E-mail: [mikko.sipila@helsinki.fi](mailto:mikko.sipila@helsinki.fi)

*New Journal of Physics* **9** (2007) 368

Received 21 June 2007

Published 9 October 2007

Online at <http://www.njp.org/>

doi:10.1088/1367-2630/9/10/368

**Abstract.** We report on the observation of two-photon electron emission from silver nanoparticles suspended in nitrogen flow resulting from irradiating them with continuous wave and pulsed laser light with photon energies below the threshold of the single-photon photoelectric effect. The photoelectron yield is quadratic in the light intensity, and the two-photon electron emission threshold is evident. The efficiency of the two-photon photoelectric effect is determined for nanoparticles of various sizes. These experiments offer the net information on nonlinear quantum properties of an isolated single nanoparticle which is crucial for developing theoretical models.

The phenomenon of the single-photon photoelectric effect ignited the development of the quantum theory of atoms, molecules, and condensed matter [1]. Detailed experimental studies of this fundamental phenomenon were performed already in the first half of 20th century. The studies of photoelectric effect on aerosol particles appeared much later, a quarter of century ago [2]–[5]. The importance of this effect on aerosols is clear, because charged particles play an important role in the atmosphere (for example, lightning, ball lightning, corona discharges and losses of electricity on high-power transmission lines). The threshold nature of the single-photon photoelectric effect limits its use at long wavelengths; however, electron photodetachment is

possible below the energy threshold due to simultaneous absorption of several photons. Even though the two-photon photoelectric effect can potentially occur in atmospheric conditions, our main motivation was a quantitative study of this effect for development of the corresponding fundamental theories.

The two-photon photoelectric effect was discovered half a century ago [6]–[8]. In recent years, two-photon photoemission spectroscopy has become a valuable tool for obtaining information about interfaces and electron dynamics [9]–[13]. The two-photon photoelectric effect on metallic nanoparticles is of interest for many practical and fundamental reasons. Of special importance are the experimental studies of this effect because of regular disagreements between theoretical predictions and the experimental results on multi-photon effects. This situation insistently demands new theoretical efforts and new measurements for creating adequate models of nonlinear interactions of nanoparticles with external electromagnetic fields. Our present study advances the progress in this direction.

The observation of the two-photon photoelectric effect on small particles is a challenging experimental task, first of all, because the effect is expected to be very weak. The known multi-photon experiments have been performed either with the particles on substrates or on rough surfaces [10]–[19]. To our knowledge, no experimental studies of the two-photon photoelectric effect from isolated nanoparticles have been reported, although the results on the single-photon photoelectric effect from aerosol particles appeared fairly long ago [2]–[5]. The advantages of measurements on isolated particles are clear. In contrast to the island film experiments, where the photocurrent from a substrate covered with particles is studied, the aerosol measurements allow one to record the charging events from individual particles. As another apparent advantage, all indefinite factors related to the substrate are removed. In practice, it is possible to measure the quantum charging efficiency of a single nanoparticle.

The main objective of the present work is to detect photoionization of separated silver nanoparticles at excitation energies below the single-photon electron emission threshold. In order to prove the two-photon nature of the effect we will have (i) to observe the quadratic dependence of the nanoparticle ionization rate on the light intensity and (ii) to demonstrate the presence of the proper threshold in the dependence of the particle ionization rate on the photon energy. It is important to determine the effect of particle size on the ionization probability.

In the experiments we used spherical silver particles of 6–24 nm in diameter generated in a tube furnace (see figure 1). Silver was chosen because it has low ionization threshold that should ease the observation of the effect, and generation methods of silver aerosol particles are well established. Silver is also a traditional and well studied material. The formed particles passed through a radioactive ( $\text{Am}^{241}$ ) neutralizer and then an electric filter which removed the remaining charged particles. The neutral particles suspended in nitrogen flow (purity 99.999%) then reached the inlet of the chamber that was a 60-cm-long channel of rectangular cross-section  $8\text{ mm} \times 8\text{ mm}$ . The transverse alternating electric field prevented recombination of charged particles and free electrons after light-induced ionization. The voltage and the frequency were chosen in such a way that free electrons and secondary negative ions were removed from the flow, with the charged silver particles being practically unaffected. Nitrogen was used as the carrier gas because it does not form negative ions in collisions with free electrons. The charged particles were separated using their electrical mobility (related to particle size) by a differential mobility analyzer (DMA, TSI-3076 or Hauke) and then detected by a condensation particle counter (TSI-3025A) (for an introduction to aerosol detection, see e.g. [20]). Total particle

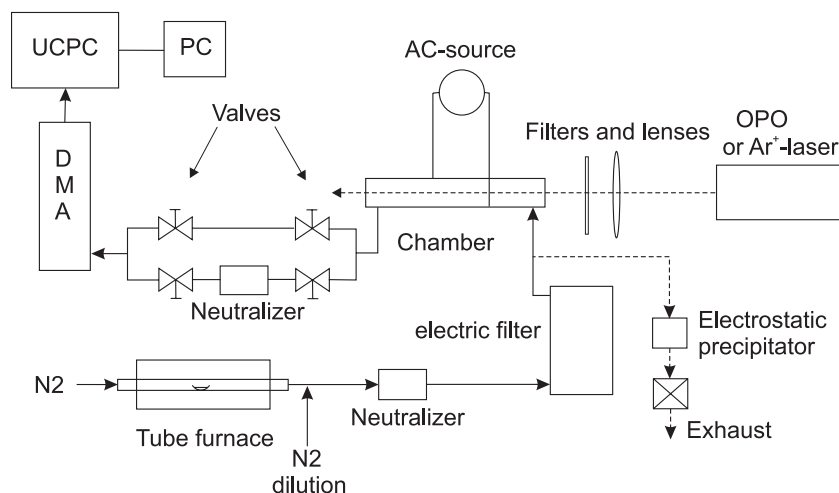


**Figure 1.** Experimental set-up. Silver nanoparticles formed in the furnace and then neutralized pass the chamber where they interact with the laser beam. The light-produced charged particles are extracted from the flow using a size selective differential mobility analyzer (DMA) and counted with an ultrafine condensation particle counter (UCPC).

fluxes for different sizes were measured using another neutralizer, in which the aerosol attains a known charge distribution [21], prior to the DMA. As an additional test, the silver particles were collected on a grid and analyzed under an electron microscope to ensure their spherical shape and exclude the presence of agglomerates which might lead to collective effects of closed packed nanoparticles [22] (figure 2).

In the first group of experiments, the aerosol particles were illuminated by the continuous wave (CW) light of an argon-ion laser (Omnichrome 543-AP, 488 nm, maximal power 160 mW). The laser beam focussed by a lens with a focal length of 650 mm was directed along the chamber. Without laser irradiation, the detected signal (due to cosmic radiation, etc) was very small ( $\sim 0.1$  particles  $\text{cm}^{-3}$ ). The signal increased enormously upon laser excitation at 488 nm, which is well below the single-photon ionization threshold ( $\sim 265$  nm for bulk silver). The signal was  $\sim 15$  particles  $\text{cm}^{-3}$  for the full (160-mW) laser power and 12 nm particles.

The photoelectric effect can be characterized by charging probability  $J_+/J_0$ , where  $J_0$  is the total particle number concentration (particles  $\text{cm}^{-3}$ ) and  $J_+$  is the number concentration of charged particles at the outlet of the reaction chamber. The charging probability as a function of the square of laser power,  $Q^2$ , is shown in figure 3 for the 488-nm CW excitation. It is seen that the effect is proportional to  $Q^2$  for all particle diameters, and this is the first indication of the two-photon process.

In another series of experiments, the aerosol particles in the reaction chamber were illuminated by 5-ns pulses of narrowband tuneable light from an optical parametric oscillator (OPO Sunlite, Continuum) with pulse energy up to approximately 0.1 mJ (inside the chamber). The 463–593 nm spectral range was scanned. In these experiments, the threshold of the electron emission was found at  $\sim 520$  nm (see below), providing thus the second strong support for the two-photon process. Indeed, this wavelength is approximately two times longer than the wavelength corresponding to the single-photon photoemission threshold of

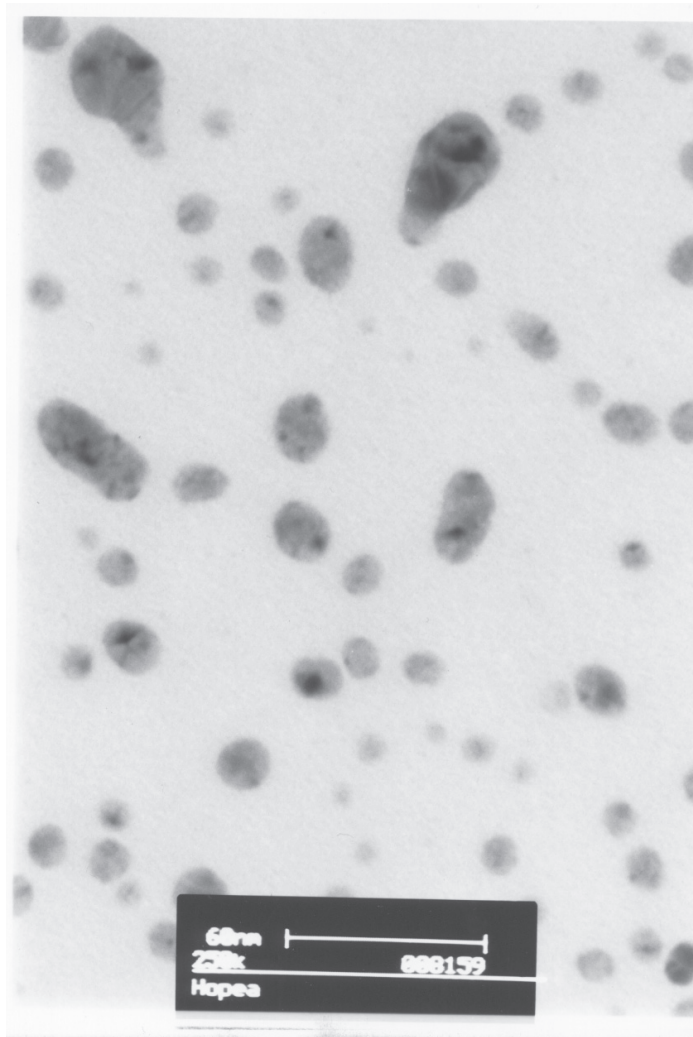


**Figure 2.** An electron microscope view of silver nanoparticles used in the experiments. Scale is 60 nm. Particles are mainly spherical up to diameters of about 20 nm and agglomerates are rare. At about 25 nm some agglomerates are present and particles larger than 30 nm (not used in the experiments) are almost completely agglomerated.

silver. In addition, the quadratic dependence of the particle charging probability on the laser intensity was confirmed for much higher light intensities than previously. Thus, the quadratic intensity dependence of the charging probability is valid at least within three orders of intensity magnitude (from  $10^2 \text{ W cm}^{-2}$  for CW light to  $>10^5 \text{ W cm}^{-2}$  for pulsed light), which is a very convincing fact.

It is important to extract from the experimental data for charging probability the absolute charging efficiency  $\gamma$  ( $\text{s}^5 \text{ g}^{-2}$ ) because this quantity can be evaluated theoretically. For the two-photon process, the charging efficiency is expressed in terms of the charging probability per unit time  $w_2$  as

$$w_2(r, z) = \gamma I^2(r, z), \quad (1)$$

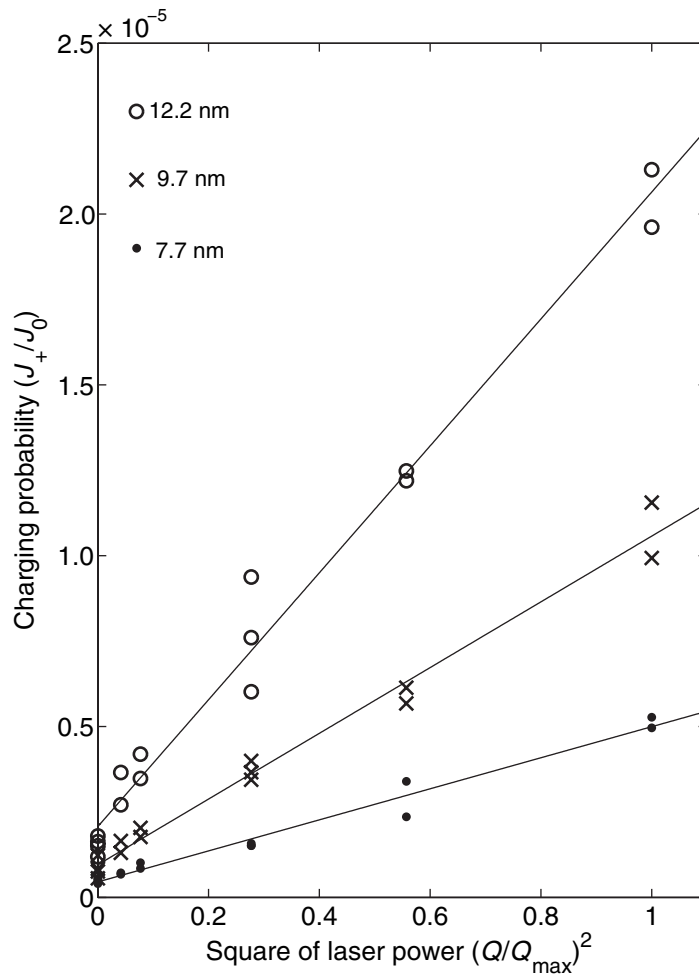


**Figure 3.** Charging probability versus the square of argon-ion laser power (488 nm). The quadratic dependence of the charging efficiency on the laser power shows the two-photon nature of the process. Four neutral filters with attenuation factors of 1.34, 1.9, 3.4 and 4.9 were used to change the excitation power.

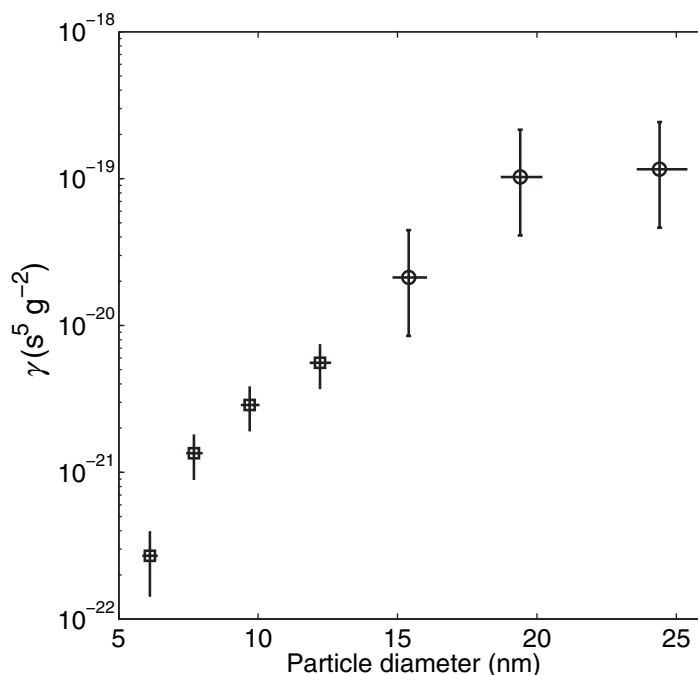
where  $I(r, t)$  is the laser intensity. For the CW excitation, the charging probability measured experimentally is written as

$$\frac{J_+}{J_0} = \frac{Q^2 \gamma}{2\pi V} \int_0^L \frac{dz}{r_0^2(z)}, \quad (2)$$

where  $V$  is the volumetric flow rate and  $r_0(z)$  is the laser beam radius that depends on  $z$  due to focusing. For pulsed excitation, the expression becomes

$$\frac{J_+}{J_0} = \gamma f T C \int I^2(t) dt, \quad (3)$$

where  $I(t)$  is the time-dependent beam intensity,  $C$  is the ratio of the irradiated volume flow and the total volume flow through the chamber,  $f$  is the repetition rate (10 Hz), and  $T$  is the time of flight through the chamber.



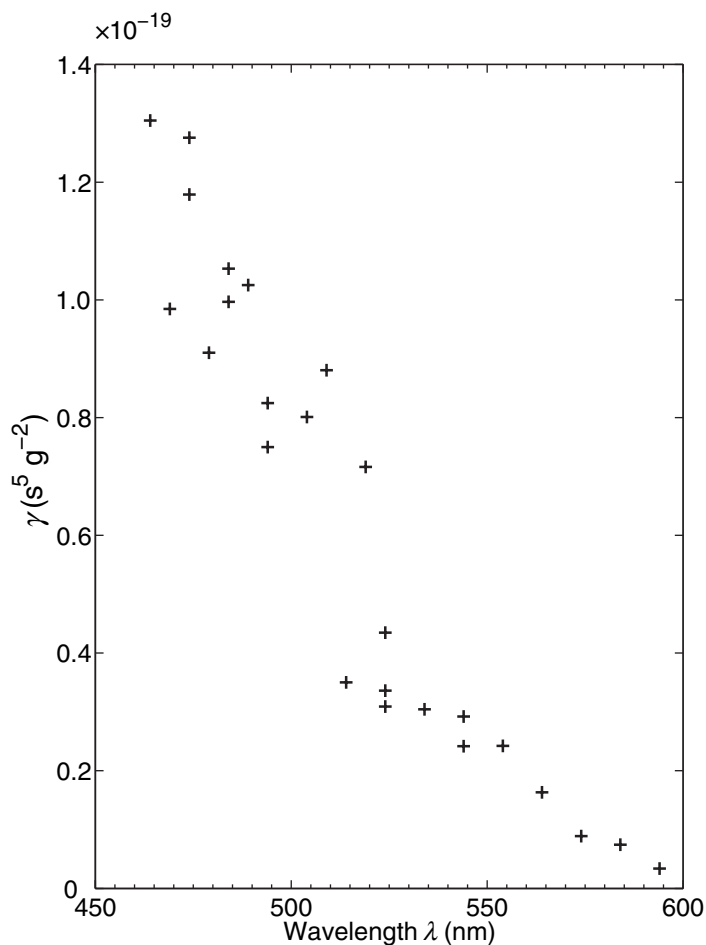
**Figure 4.** Charging efficiency of two-photon photoelectric effect versus particle size at  $\lambda = 488$  nm. The data were obtained with CW (squares) and pulsed (circles) excitation.

Figure 4 presents the two-photon charging efficiency for various particle diameters. It summarizes the data from experiments with CW excitation (6–12 nm particles) and pulsed excitation (15–25 nm particles) at 488 nm. Both the experiments perfectly agree with each other. The size dependence is more pronounced than in the case of the single photon effect from silver particles [3]. Two-photon emission can occur at such low energy of incident photons only if the first photon excites  $1e-1$  h state and the second photon hits the excited particle and excites the second  $1e-1$  h state. The number of excited states  $n$  is  $n \sim w_1 \tau$ , where  $w_1$  is the rate of single photon absorption and  $\tau$  is the lifetime of  $1e-1$  h state.

A free electron appears after the Coulomb interaction has redistributed the energy of the thus formed  $2e-2$  h state in such a way that one of the excited electrons would have an energy above the photoelectron threshold. The rate of the two photon process is thus  $w_2 \sim n w_1 = w_1^2 \tau$ . Next, for small particles  $w_1 \sim d^3$ , where  $d$  is the particle diameter. Unfortunately, no reasonable estimate of  $\tau$  exists so far. Most likely this time does not depend on the particle size (because it is related to the electron–electron collisions rather than the electron–wall collisions). In this case,  $w_2 \sim d^6$ . This result overestimates the observed behavior, but clearly shows that size dependence should be stronger than in the case of the single photon process. One should also keep in mind that  $w_2$  gives an upper estimate of the photoelectron production rate and does not take into account all factors related to the electron escape. Theoretical efforts are demanded for detailed quantification of this phenomenon.

A threshold in the two-photon charging efficiency  $\gamma$  was observed at  $\sim 520$  nm when the wavelength of irradiation was varied (figure 5). The sum energy of two photons at the threshold is about 4.7 eV, which agrees with the single-photon ionization threshold of





**Figure 5.** Charging efficiency of two-photon photoelectric effect for 19 nm particles versus the wavelength of laser light. The threshold at  $\sim 520$  nm is seen.

silver nanoparticles [2]. Together with the observed quadratic intensity dependence, this result provides strong evidence in favour of the two-photon nature of the observed particle charging.

Now, we discuss the possibility of thermal effects in our experiments such as thermionic emission or semidirect photoelectric effect [23] from heated particles. For CW irradiation, the temperature of nanoparticles can be accurately derived by assuming a steady state energy balance. As a result, we obtained a possible temperature increase less than  $1^\circ\text{C}$  at the maximal laser power while for observable thermionic or semidirect photoelectric emission rates a temperature increase of at least  $\sim 1000^\circ\text{C}$  would be needed. The weakness of the laser heating effect is due to very efficient heat transfer from nanoparticles to the buffer gas [24]. For pulsed irradiation the temperature is more difficult to evaluate since uniform heating cannot be assumed. However, the matching of the results for pulsed and CW excitations indicates that the thermal contribution to the observed particle ionization is minor in the pulsed regime as well.

As a conclusion, the aerosol instrumentation used in the present work allowed us to detect for the first time two-photon charging of isolated nanoparticles. We found two strong features of the two-photon nature of the photoelectric effect: the quadratic dependence of the charging

probability on the light intensity and the suitable energy threshold of the process at  $\sim 520$  nm. We determined the two-photon charging efficiency for silver nanoparticles of various sizes. Charging efficiencies were very low even for silver with low work function compared to any atmospherically relevant compounds. Thus this phenomenon cannot significantly contribute to atmospheric charge production, even though the wavelengths used in the experiment are close to the sun spectral maximum. These results are free from collective effects (closed packed particles) or the interface between the substrate and the particle and can stimulate further theoretical development in the field. Experimental methods presented here would allow one to produce an extensive set of quantitative data on this effect also for other materials and for a wider wavelength and particle size range.

### Acknowledgment

The Academy of Finland supported this work partially through CoE CMS and the FinNano Program (OPNA).

### References

- [1] Einstein A 1905 *Ann. Phys.* **17** 132
- [2] Burtscher H, Sherrer L, Siegmann H C, Schmitt-Ott A and Federer B 1982 *J. Appl. Phys.* **53** 3787
- [3] Schmidt-Ott A and Federer B 1981 *Surf. Sci.* **106** 538
- [4] Burtscher H and Schmidt-Ott A 1985 *Surf. Sci.* **156** 735
- [5] Burtscher H and Schmidt-Ott A 1982 *Phys. Rev. Lett.* **48** 1734
- [6] Smith R L 1962 *Phys. Rev.* **128** 2225–9
- [7] Sonnenberg H, Heffner H and Spicer W 1964 *Appl. Phys. Lett.* **5** 95
- [8] Teich M C, Schroerer J M and Wolga J G 1964 *Phys. Rev. Lett.* **13** 611
- [9] Takagi Y 1994 *Appl. Opt.* **33** 6328
- [10] Ertl K, Kohl U, Merschdorf M, Pfeiffer W, Thon A, Voll S and Gerber G 1999 *Appl. Phys. B* **68** 439
- [11] Lehmann J, Merschdorf M, Pfeiffer W, Thon A, Voll S and Gerber G 2000 *J. Chem. Phys.* **112** 5428
- [12] Lehmann J, Merschdorf M, Pfeiffer W, Thon A, Voll S and Gerber G 2000 *Phys. Rev. Lett.* **85** 2921
- [13] Merschdorf M, Kennerknecht C and Pfeiffer W 2004 *Phys. Rev. B* **70** 193401
- [14] Fedorovich R D, Naumovets A G and Tomchuk P M 2000 *Phys. Rep.* **328** 73
- [15] Shalaev V M, Douketis C, Haslett T, Stuckless T and Moskovits M 1996 *Phys. Rev. B* **53** 11193
- [16] Drachev V P, Khaliullin E N, Kim W, Alzoubi F, Rautian S G, Safonov V P, Armstrong R L and Shalaev V M 2004 *Phys. Rev. B* **69** 035318
- [17] Varró S and Ehlotzky F 1997 *J. Phys. D: Appl. Phys.* **30** 3071
- [18] Sabary F, Dudek J C and Bergeret H 1991 *J. Appl. Phys.* **70** 1066
- [19] Monchicourt P, Raynaud M, Saringar H and Kupersztych J 1997 *J. Phys. C: Condens. Matter* **9** 5765
- [20] Aalto P *et al* 2001 *Tellus B* **53** 344
- [21] Wiedensohler A 1990 Die bibolare Diffusionsaufladung von Partikeln in chemisch tragen Reinsstgasen  
*PhD Thesis* University of Duisburg
- [22] Khriachtchev L, Heikkilä L and Kuusela T 2001 *Appl. Phys. Lett.* **78** 1994
- [23] Lushnikov A A and Negin A E 1992 *J. Aerosol Sci.* **24** 707
- [24] Williams M M R and Loyalka S K 1991 *Aerosol Science: Theory and Practice* (Oxford: Pergamon)